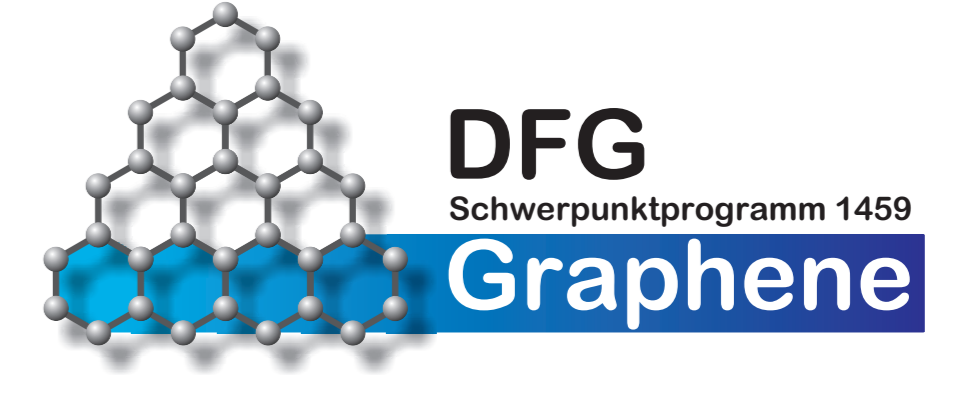# Scattering of 2D Dirac fermions on gate-defined oscillating quantum dots

Christian Schulz, Rafael Leslie Heinisch, and Holger Fehske
Institute of Physics, University Greifswald, Germany

DFG
Schwerpunktprogramm 1459
Graphene

Abstract

Within an effective Dirac-Weyl theory we solve the scattering problem for massless chiral fermions impinging on a cylindrical time-dependent potential barrier. The setup we consider can be used to model the electron propagation in a monolayer of graphene with harmonically driven quantum dots. For static small-sized quantum dots scattering resonances enable particle confinement and interference effects may switch forward scattering on and off. An oscillating dot may cause inelastic scattering by excitation of states with energies shifted by integer multiples of the oscillation frequency, which significantly modifies the scattering characteristics of static dots. Exemplarily the scattering efficiency of a potential barrier with zero bias remains finite in the limit of low particle energies and small potential amplitudes. For an oscillating quantum dot with finite bias, the partial wave resonances at higher energies are smeared out for small frequencies or large oscillation amplitudes, thereby dissolving the quasibound states at the quantum dot.

Model & solution of the scattering problem

- 2D Dirac-Weyl equation in graphene

$$i\partial_t\psi(r,t) = -i\boldsymbol{\sigma}\boldsymbol{\nabla}\psi(r,t) + \hat{U}(r,t)\psi(r,t)$$

with circular harmonically driven potential step

$$\hat{U}(r,t) = \left[V + \tilde{V}\sin\omega t\right]\theta(R-r)\hat{I}$$

neglecting intervalley scattering with low-energy approximation

- Floquet-theory + eigenfunctions (energy $n \in \mathbb{Z}$ + angular momentum $m \in \mathbb{Z}$)
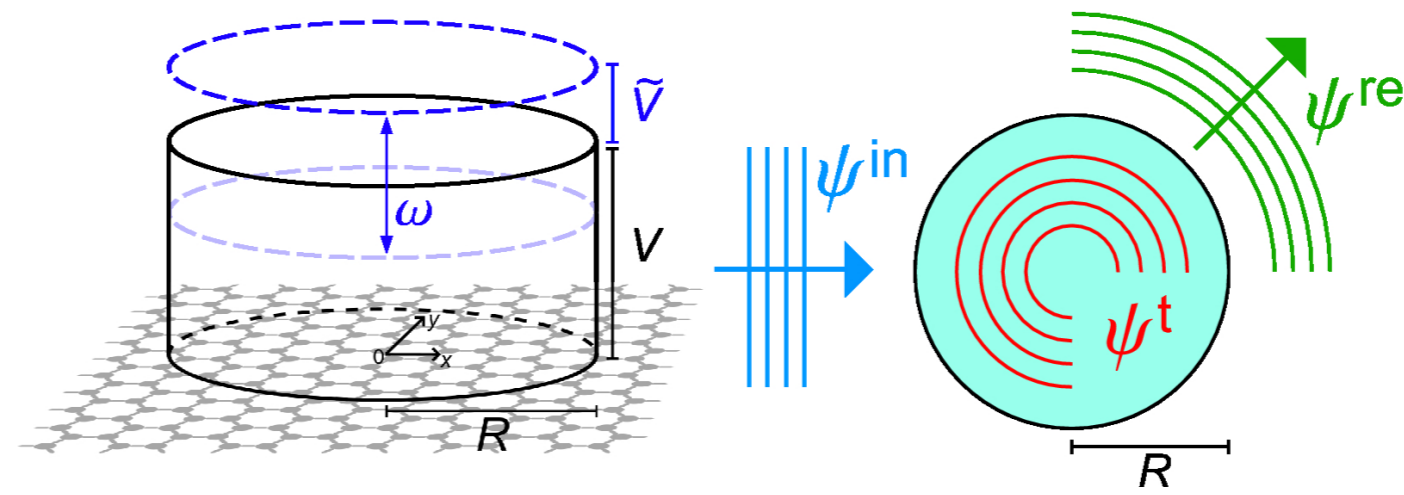- matching the wave functions at $r = R$

near-field quantities

$\rho = \psi^\dagger\psi$ particle density

$\boldsymbol{j} = \psi^\dagger\boldsymbol{\sigma}\psi$ current density

far-field quantities

$j_r^{\mathrm{ref}}(r-t,\varphi) = \psi^{\mathrm{ref}\dagger}\hat{j}_r\psi^{\mathrm{ref}}$ angular scattering

$Q(r-t) = \dfrac{1}{2R}\oint \boldsymbol{j}^{\mathrm{ref}}\mathbf{ds}$ scattering efficiency
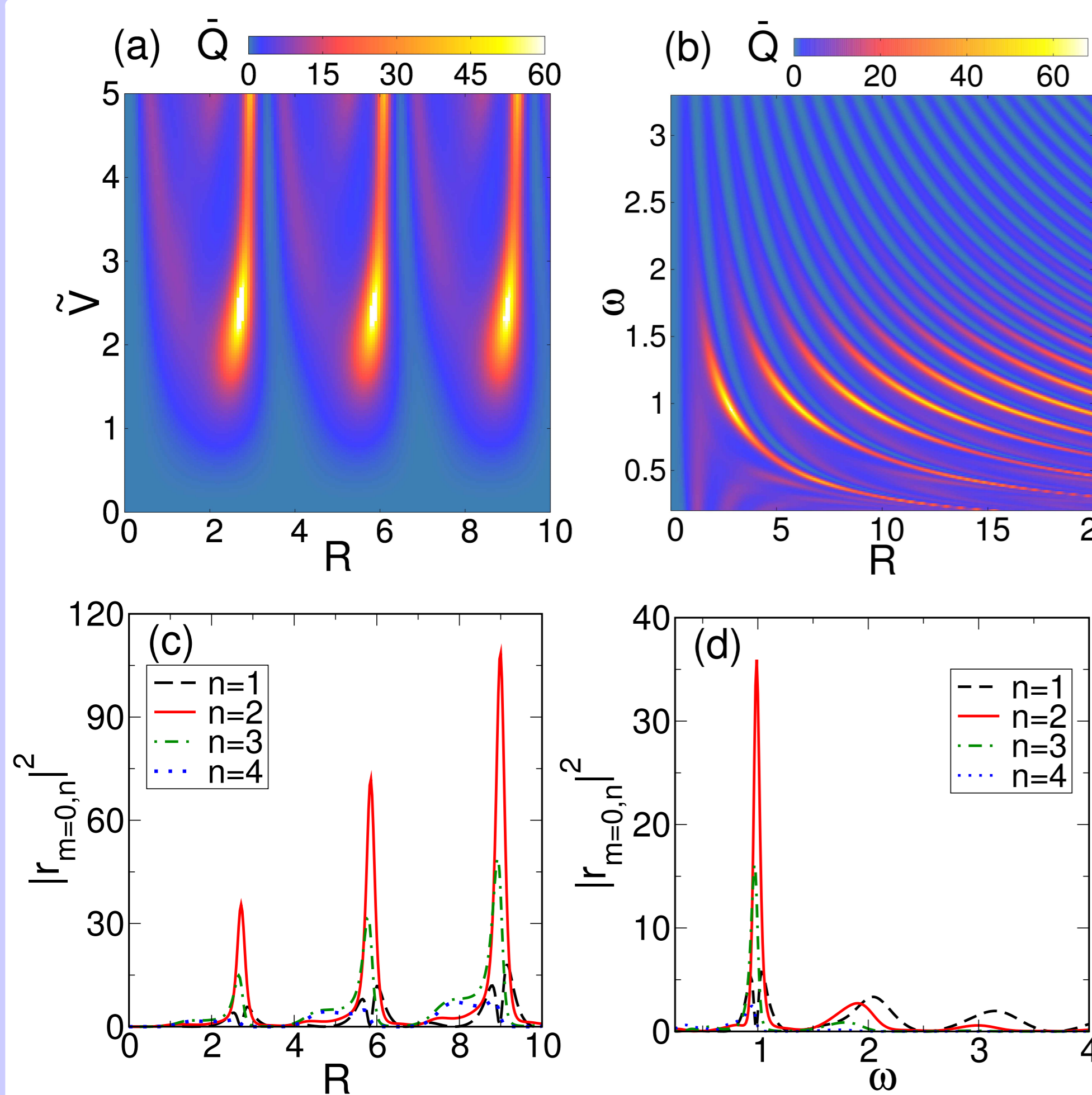
Scattering process. A low-energy plane Dirac electron wave ψ^{in}, propagating in a monolayer graphene sheet on a gated substrate, hits a circular time-dependent potential step that can be tuned by applying a voltage. The gate-defined graphene quantum dot is characterized by the constant (V) and oscillating ($\tilde{V},\omega$) parts of the potential, and the radius R. In the process of scattering reflected ψ^{ref} and transmitted ψ^t waves appear.
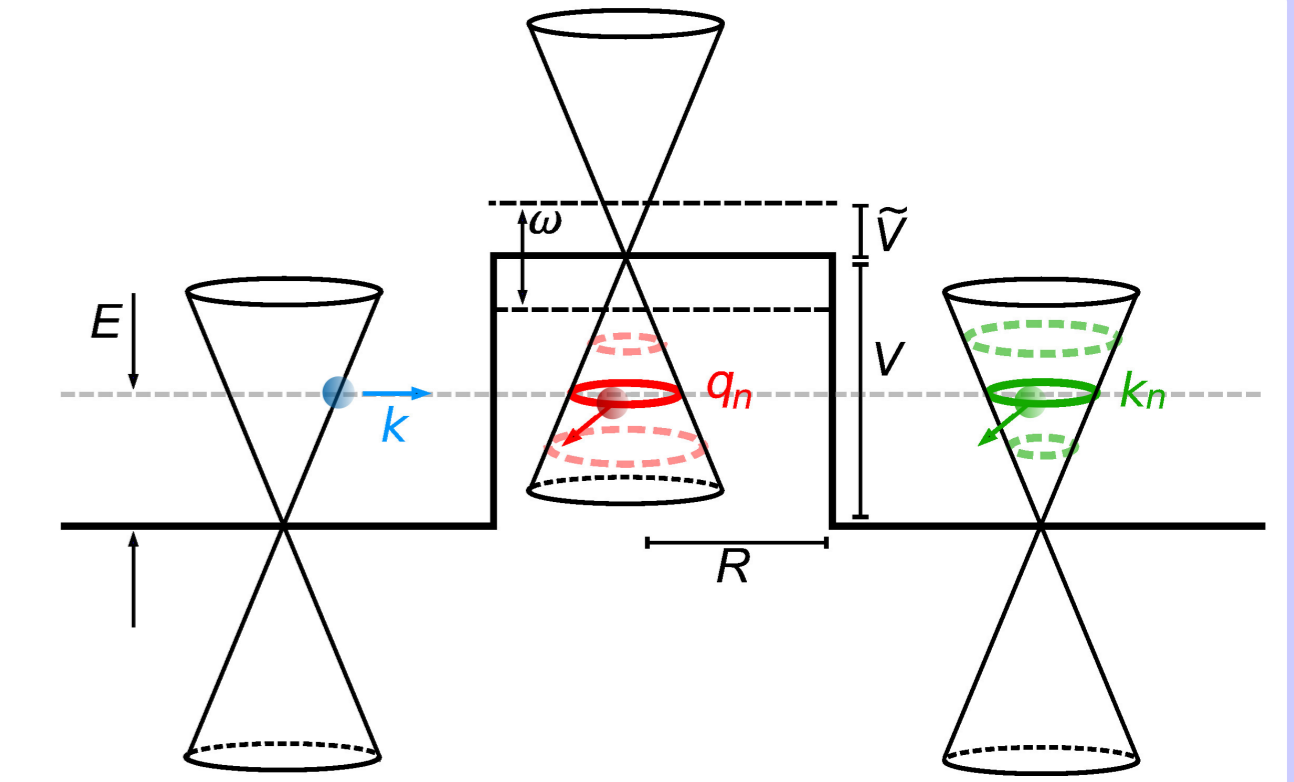
Bandstructure and energy conditions. On account of the time-dependent potential the particles energy E is not conserved. The reflected and transmitted particles have quantized energies, $E_n = E + n\omega$ where $n = 0, \pm 1, \pm 2, \dots$ (only the first excited energies were marked in the plot), and carry an angular momentum (i.e., their wave vectors have components in any planar direction).
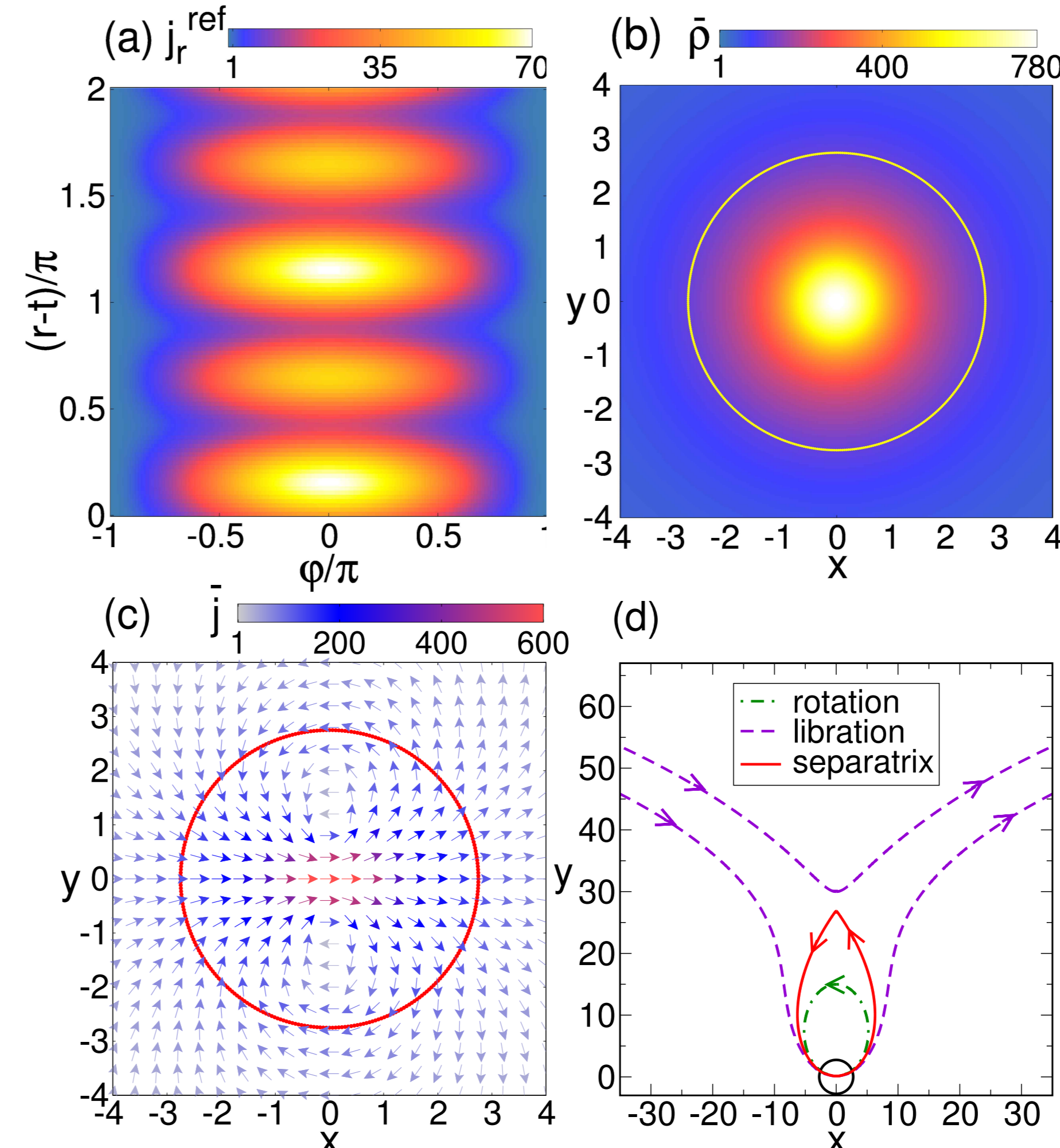
Quantum dot with zero bias

(a) $\bar{Q}$ 0 15 30 45 60

(b) $\bar{Q}$ 0 20 40 60

(c) |$r_{m=0,n}$|^2 n=1, n=2, n=3, n=4

(d) |$r_{m=0,n}$|^2 n=1, n=2, n=3, n=4

scattering behavior

- near the charge neutrality point (with zero bias): resonance of partial waves with $m = 0$ ($n \neq 0$) only
- "absorption threshold": $\tilde{V}/\omega \approx 1$
- pronounced scattering signals: quasibound states at the quantum dot
- peaks in $\bar{Q}$ are determined by peaks of the scattering coefficients $|r_{m=0,n\neq0}|^2$
- dot act as a switch: scattering can be turned on and off by varying frequency ω at fixed $R, \tilde{V}$

limiting cases

1. "static regime" $\tilde{V} \to 0$
2. "adiabatic regime" $\omega \to 0$: the smaller ω the more dot eigenmodes can be excited; scattering becomes completely inelastic
3. "antiadiabatic regime" $\omega \to \infty$: particle feels an averaged potential only

$\Rightarrow$ scattering efficiency vanishes

Scattering efficiency. Intensity plot of the time-averaged far-field scattering efficiency $\bar{Q}$ of an oscillating graphene quantum dot with $V = 0$ near the charge neutrality point $E = 0$, as function of R and $\tilde{V}$ for $\omega = 1$ [panel (a)], respectively, in dependence on R and ω for $\tilde{V} = 2.32$ [panel (b)]. Panels (c) and (d) give the first four scattering coefficients $|r_{m=0,n}|^2$ of the reflected wave for $\tilde{V} = 2.32$, $\omega = 1$ and for $R = 2.75$, $\tilde{V} = 2.32$, respectively. The pattern of the scattering efficiency is determined by the scattering coefficients with $m = 0$, $n \neq 0$.

(a) j_r^{ref} 1 35 70

(b) $\bar{\rho}$ 1 400 780

(c) $\bar{\jmath}$ 200 400 600

(d) rotation, libration, separatrix

scattering characteristics

- forward scattering is preferred (resonance of $m = 0$ mode only)
- symmetry $|r_{0,n}| = |r_{0,-n}|$: period of emittance is half the period of the potential oscillation

near field

- incident electron is temporarily captured by the quantum dot and subsequently reemitted in forward direction
- maximum electron density in the center of the quantum dot at $r = 0$ (partial trapping of the particle)
- pattern of the current density is symmetric to the x axis and reveals two vortices where the incident wave is fed into
- different regimes of near-field current pattern: bound (rotation) and unbound (libration) flow lines separated by a separatrix
- Klein tunneling (i.e., perfect transmittance, no backscattering) for perpendicular incidence

Radiant emittance by the quantum dot. The parameters $\tilde{V} = 2.32$, $\omega = 1$, and $R = 2.75$ used belong to a strong scattering signal. Panel (a) displays the time-dependence of the far-field radial component of the reflected current j_r^{ref}. Panels (b) and (c) show the time-averaged density $n = \psi^\dagger\psi$ and current field $\bar{\jmath} = \psi^\dagger\sigma\psi$ in the near field, respectively. Panel (d) classifies the current field: unbound librations (violet lines) and bound rotations (green curve) are separated by a separatrix (red curve).

Quantum dot with finite bias

(a) $\bar{Q}$ 0 3 6 9 12

(b) $\bar{Q}$ 0 3 6 9

(c) |$r_{m=0,n}$|^2

(d) |$r_{m=1,n}$|^2 n=0, n=1, n=-1, n=2, n=-2, n=3, n=-3
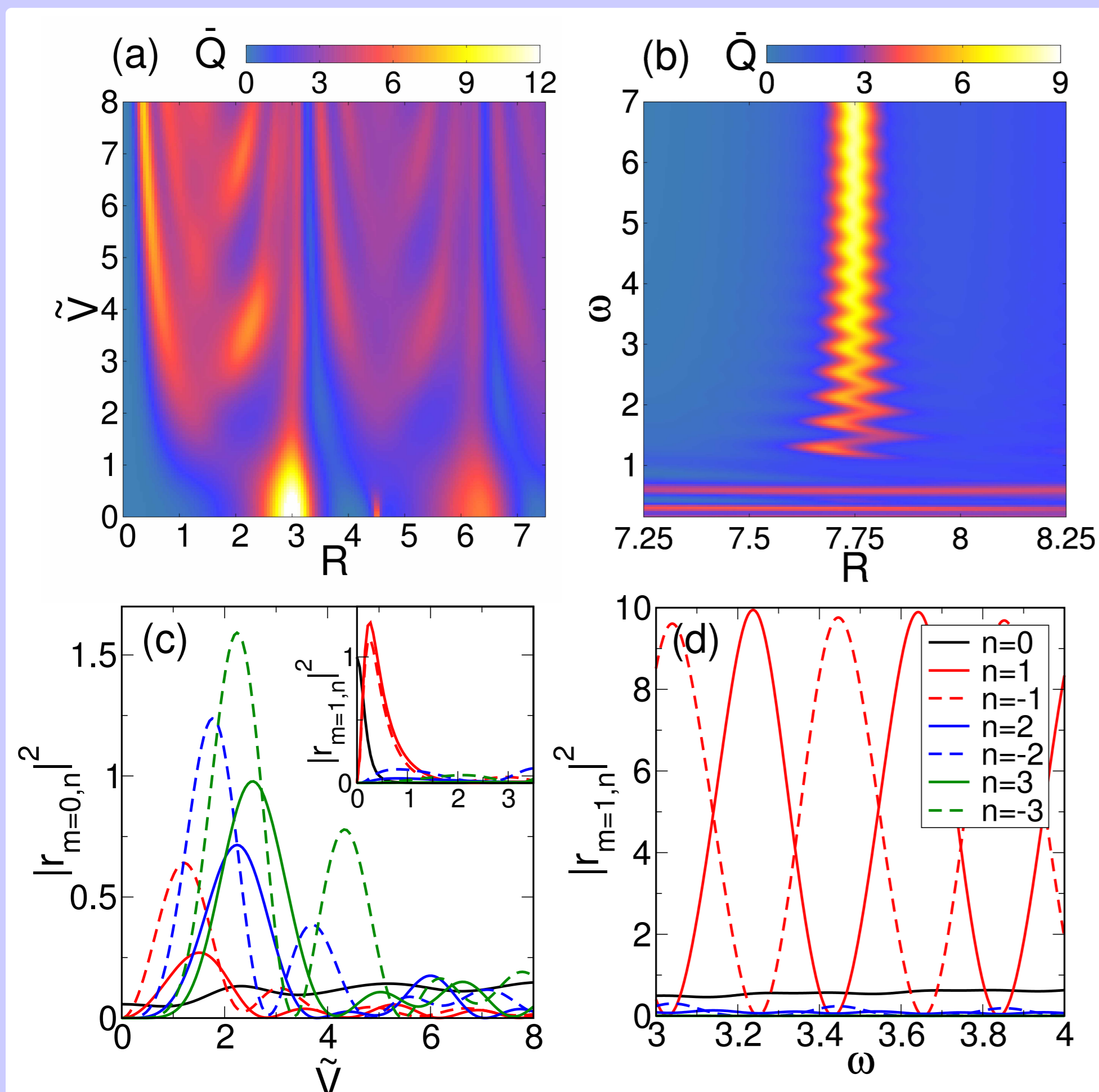
below absorption threshold

- elastic scattering for $\tilde{V}/\omega \ll 1$
- static quantum dot for $\tilde{V} \to 0$ ("static regime") and $\omega \to \infty$ ("antiadiabatic regime") $\Rightarrow$ resonances belonging to quasilocalized modes: broad $m = 0$-mode and sharp $m = 1$-mode in panel (a), $m = 1$-mode in panel (b)

above absorption threshold

- inelastic scattering for $\tilde{V}/\omega \simeq 1$: resonances with higher energies ($|n| > 0$) will be excited $\Rightarrow$ largely washed-out scattering signals as a result of superimposing of states with different n
- decreasing ω: oscillation of intensity maximum due to asymmetry of the dot potential
- "adiabatic regime" $\omega \ll \tilde{V}$: large number of dot modes are stimulated $\Rightarrow$ signatures composed of many partial waves with different m, n

Scattering efficiency. Intensity plot of the time-averaged far-field scattering efficiency $\bar{Q}$ of an oscillating graphene quantum dot with finite bias ($V = 1$), in dependence on R and $\tilde{V}$ for $\omega = 1$, $E = 0.1$ [panel (a)], respectively, as a function R and ω for $\tilde{V} = 0.75$ and $E = 0.0629$ [panel (b)]. The lower figures give the corresponding (squared) amplitudes of the scattering coefficients $|r_{m,n}|^2$ as functions of $\tilde{V}$ [panel (c), where $E = 0.1$, $\omega = 1$, $R = 4.5$] and ω [panel (d)], where $E = 0.0629$, $\tilde{V} = 0.75$, $R = 7.75$] of the reflected wave.

Zero-frequency Limit

(a) $\bar{Q}$ 0 5 10

(b) Q^{st} 0.1 1 10 100

(c) $\bar{Q}$ r_0^{st}, r_1^{st}, r_2^{st}, $\omega \to 0$, $\omega = 0.15$
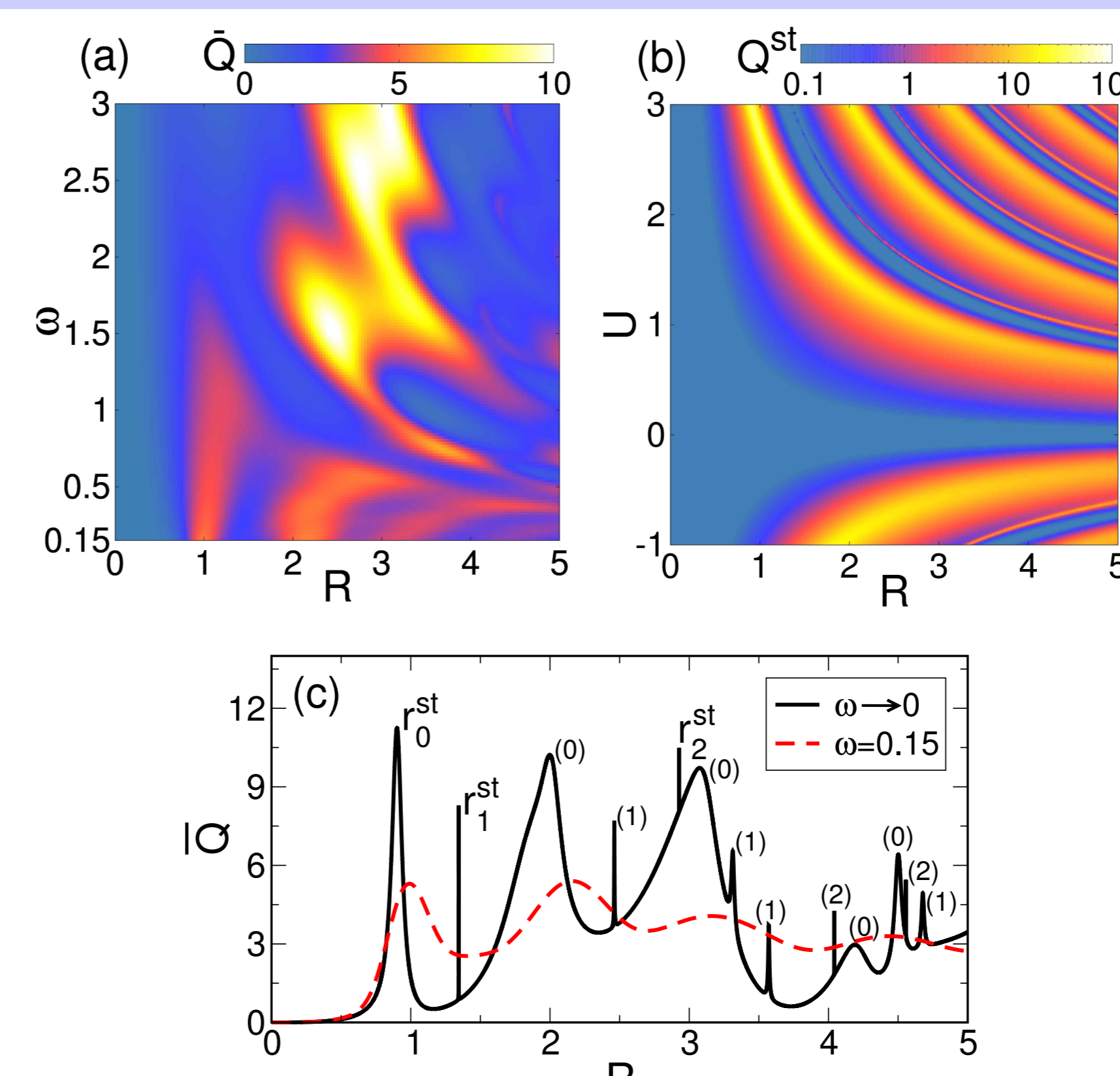
near the "adiabatic" regime $\omega \to 0$: large number of possibly excited energy levels $\Rightarrow$ numerical treatment cumbersome!

analytical approach

- static quantum dot at any infinitesimal point in time τ

$$Q^{\mathrm{st}}[U] = \frac{4}{kR}\sum_{m=0}^{\infty}\left|r_m^{\mathrm{st}}(U)\right|^2$$

with $U = V + \tilde{V}\sin(\omega\tau)$

- scattering efficiency in the adiabatic limit:

$$\bar{Q}(\omega \to 0) = \frac{1}{2\tilde{V}}\int_{V-\tilde{V}}^{V+\tilde{V}} Q^{\mathrm{st}}[U]\,dU$$

- adiabatic structures in scattering efficiency can be associated to the static dot's $m = 0$ mode and its overtones

Scattering behavior approaching the adiabatic limit. System parameters are $E = 0.1$, $V = 1$, and $\tilde{V} = 2$. (a) Time-averaged scattering efficiency $\bar{Q}$ as function of R and ω. (b) Static scattering efficiency $Q^{\mathrm{st}}[U]$. (c) Time-averaged scattering efficiency $\bar{Q}$ at fixed $\omega = 0.15$ (red curve) compared to the result $\bar{Q}(\omega \to 0)$ obtained in the adiabatic limit (black line).

Conclusions

- above absorption threshold $\tilde{V}/\omega \approx 1$: inelastic scattering with potential transitions into side-bands $E_n = E + n\omega$.
- antiadiabatic ($\omega \gg \tilde{V}$): elastic scattering (static quantum dot), adiabatic ($\omega \ll \tilde{V}$): completely inelastic scattering.
- Zero-bias case (near the charge neutrality point): enhanced forward scattering, periodic emittance/trapping by the quantum dot, dot act as a switch by tuning the dot parameters R, ω and $\tilde{V}$.
- Finite-bias case: modes with finite angular momentum & excited (shifted) energies belonging to side bands with positive and negative n, largely out-washed and oscillating scattering signals above the absorption threshold $\tilde{V}/\omega \approx 1$.

[1] C. Schulz, R. L. Heinisch, and H. Fehske, Phy. Rev. B 91, 045130 (2015).
[2] C. Schulz, R. L. Heinisch, and H. Fehske, Quantum Matter, arXiv:1412.2539v1 (2014).
[3] R. L. Heinisch, F. X. Bronold, and H. Fehske, Phy. Rev. B 87, 155409 (2013).